2016

# Evaluating energy consumption of air gap membrane distillation for seawater desalination at pilot scale level

Hung Duong
*University of Wollongong*, chd581@uowmail.edu.au

Paul Cooper
*University of Wollongong*, pcooper@uow.edu.au

Bart Nelemans
*AquaStill*

Tzahi Y. Cath
*Colorado School Of Mines*, tcath@mines.edu

Long D. Nghiem
*University of Wollongong*, longn@uow.edu.au

# Evaluating energy consumption of air gap membrane distillation for seawater desalination at pilot scale level

**Abstract**

This study aimed to optimise an air gap membrane distillation (AGMD) system for seawater desalination with respect to distillate production as well as thermal and electrical energy consumption. Pilot evaluation data shows a notable influence of evaporator inlet temperature and water circulation rate on process performance. An increase in both distillate production rate and energy efficiency could be obtained by increasing the evaporator inlet temperature. On the other hand, there was a trade-off between the distillate production rate and energy efficiency when the water circulation rate varied. Increasing the water circulation rate resulted in an improvement in the distillate production rate, but also an increase in both specific thermal and electrical energy consumption. Given the small driving force used in the pilot AGMD, discernible impact of feed salinity on process performance could be observed, while the effects of temperature and concentration polarisation were small. At the optimum operating conditions identified in this study, a stable AGMD operation for seawater desalination could be achieved with specific thermal and electrical energy consumption of 90 and 0.13 kW h/m3, respectively. These values demonstrate the commercial viability of AGMD for small-scale and off-grid seawater desalination where solar thermal or low-grade heat sources are readily available.

**Keywords**

scale, pilot, desalination, seawater, distillation, membrane, gap, air, level, consumption, evaluating, energy

**Disciplines**

Engineering | Science and Technology Studies

# Evaluating energy consumption of air gap membrane distillation for seawater desalination at pilot scale level

Submitted to

**Separation and Purification Technology**

Hung C. Duong[a], Paul Cooper[b], Bart Nelemans[c], Tzahi Y. Cath[d], Long D. Nghiem[a,*]

[a] Strategic Water Infrastructure Laboratory, School of Civil Mining and Environmental Engineering, University of Wollongong, Wollongong, NSW 2522, Australia

[b] Sustainable Buildings Research Centre, University of Wollongong, Fairy Meadow, NSW 2519, Australia

[c] AquaStill, Nusterweg 69, 6136 KT Sittard, The Netherlands

[d] Advanced Water Technology Center (AQWATEC), Department of Civil and Environmental Engineering, Colorado School of Mines, Golden, CO 80401, USA

_____

* Corresponding author: Long Duc Nghiem, Email longn@uow.edu.au; Tel: +61 2 4221 4590

**Abstract:** This study aimed to optimise an air gap membrane distillation (AGMD) process for seawater desalination with respect to distillate production as well as thermal and electrical energy consumption. Pilot evaluation data shows a notable influence of evaporator inlet temperature and water circulation rate on process performance. An increase in both distillate production rate and energy efficiency could be obtained by increasing the evaporator inlet temperature. On the other hand, there was a trade-off between the distillate production rate and energy efficiency when the water circulation rate varied. Increasing the water circulation rate resulted in an improvement in the distillate production rate, but also an increase in both specific thermal and electrical energy consumption. Given the small driving force used in the pilot AGMD, discernible impact of feed salinity on process performance could be observed, while the effects of temperature and concentration polarisation were small. At the optimum operating conditions identified in this study, a stable AGMD operation for seawater desalination could be achieved with specific thermal and electrical energy consumption of 90 and 0.13 kWh/m$^3$, respectively. These values demonstrate the commercial viability of AGMD for small-scale and off-grid seawater desalination where solar thermal or low-grade heat sources are readily available.

*Keywords:* membrane distillation; air gap membrane distillation (AGMD); energy consumption; seawater desalination; process optimisation.

# 1. Introduction

Desalination is a practical approach to increase and secure drinking water supply in coastal areas [1]. Drinking water supply from seawater using large-scale reverse osmosis (RO) and conventional thermal distillation has been implemented in many parts of the world. However, the provision of drinking water to small and remote coastal communities remains a significant challenge. Conventional thermal distillation is less energy efficient and requires a larger physical footprint compared to RO. On the other hand, RO, as a pressure-driven membrane separation process, requires intensive pre-treatment, high-pressure pumps, and duplex stainless steel piping. As a result, RO may not be suitable for small-scale seawater desalination applications, particularly in areas with unreliable or limited power supply. In this context, membrane distillation (MD), given its ability to use solar thermal and low-grade heat directly as the primary source of energy, has been identified as a potential candidate for small-scale and off-grid seawater desalination applications [2-5].

MD is combination of membrane separation and phase-change thermal distillation [6, 7]. In MD, a hydrophobic, microporous membrane is used as a barrier against the liquid phase, but allows the vapour phase (i.e., water vapour) to pass through. As a result, MD, like a conventional thermal distillation process, can offer ultrapure water directly from seawater. MD can also retain most advantages of a typical membrane process, including modulation, compactness, and process efficiency [6, 7]. Thus, the physical and energy footprints of MD can be lower than those of conventional thermal distillation [8, 9]. In addition, given the absence of a high hydraulic pressure and the discontinuity of the liquid phrase across its membrane, MD is less susceptible to membrane fouling and does not require intensive feed water pre-treatment compared to RO [6, 10]. More importantly, MD systems can be manufactured from non-corrosive and inexpensive plastic materials, leading to significantly reduced capital and maintenance costs. Finally, the feed operating temperature of MD is often in the range of 40 to 80 ℃, which is also the optimal operating temperature with respect to thermal efficiency of most thermal solar collectors [11]. Given these attributes, MD is a promising candidate for small-scale, stand-alone, and solar-driven seawater desalination applications [3, 11-13].

Despite a range of attributes that are highly suitable for small-scale and off-grid seawater desalination, there are still several technical challenges to the practical realisation of MD.

Amongst them, low thermal efficiency is the most considerable. As a thermally driven separation process, MD requires huge amounts of thermal energy to facilitate the phase conversion of liquid water into vapour, and vice versa. As a result, the specific energy consumption of all MD processes reported in the literature to date is several orders of magnitude higher than that of RO [4, 12, 14].

MD can be operated in four basic configurations, including direct contact membrane distillation (DCMD), sweeping gas membrane distillation (SGMD), vacuum membrane distillation (VMD), and air gap membrane distillation (AGMD). DCMD has the lowest thermal efficiency due to significant heat conduction through the membrane. In SGMD and VMD, the introduction of sweeping gas and vacuum, respectively, mitigates the heat loss due to conduction, and hence improves the process thermal efficiency. However, this also increases the process complexity because an external condenser must be employed to obtain fresh water, thus limiting the practical applications of SGMD and VMD for seawater desalination. AGMD has a higher thermal efficiency compared to DCMD but lower process complexity compared to SGMD and VMD. Therefore, AGMD has been the most widely studied configuration for seawater MD desalination at pilot-scale level [15-17].

In AGMD, a stagnant air gap is maintained between the membrane and the condenser channel by using a condenser foil. The stagnant air gap functions as a thermal insulation layer. As a result, the heat loss due to conduction, which is intrinsic to DCMD, is noticeably reduced in AGMD. Moreover, because the distillate and coolant are separated by the condenser foil, in a single-pass AGMD process seawater at ambient temperature can be used as the coolant prior to being externally heated and fed into the evaporator channel. The latent heat of condensation can be recovered to pre-heat the feed, thus reducing the thermal energy consumption of AGMD [10, 18, 19]. It is noteworthy that amongst the aforementioned configurations, only AGMD permits the latent heat recovery without an external heat exchanger. In addition, cooling, which must be used in other configurations, can be excluded in single-pass AGMD, hence further reducing its thermal energy consumption. However, the stagnant air gap also increases the overall resistance to mass transfer; therefore, AGMD is usually operated at a lower water flux compared to other configurations [16, 17, 20].

To date, there have been only few studies on process optimisation of AGMD desalination at pilot-scale with respect to distillate production and thermal and especially electrical energy

consumption. As a notable example, Guillen-Burrieza et al. [15] investigated the performance of two pilot-scale AGMD systems using synthetic NaCl solutions as the feed. They elucidated the influences of feed inlet temperature and water circulation rate on water flux, distillate quality, and thermal energy consumption of the systems. However, they did not consider membrane fouling propensity and electrical energy consumption [15]. Koschikowski et al. [10] reported experimental investigations on eight stand-alone, solar-powered pilot AGMD systems for drinking water production from seawater. The distillate production rate of the systems for one typical day and for over three years of operation was evaluated. Nevertheless, Koschikowski et al. [10] did not assess the energy consumption of their systems.

Given the significant research gap with respect to the optimisation of energy consumption and water production rate of AGMD for seawater desalination, this study aims at elucidating the influences of operating conditions on the performance and thermal and electrical energy consumption of a single-pass, pilot-scale AGMD process. The effects of temperature and concentration polarisation effects and feed salinity on distillate production rate and energy consumption of the process were analysed. The feasibility of a single-pass pilot AGMD to produce fresh water from actual seawater without any pre-treatment was also demonstrated.

## 2. Materials and methods

### 2.1. Materials

#### 2.1.1. Pilot AGMD system

A pilot AGMD system (Fig. 1) was used. The system consisted of a spiral-wound AGMD membrane module (Aquastill, Sittard, The Netherlands), a feed tank, a water-circulating pump, temperature and pressure sensors, and a magnetic flow meter. The spiral-wound membrane module had 6 evaporator channels, 6 condenser channels, and 12 distillate channels. Each evaporator channel was formed with microporous low-density polyethylene (LDPE) membranes with nominal pore size of 0.3 μm, thickness of 76 μm, and porosity of 85%. Coated aluminium foils were used to create the condenser channels. Mesh spacers, 1 mm in thickness, were inserted between the evaporator channels and condenser channels to create the distillate channels. Mesh spacers with thickness of 2 mm were also used in the evaporator and condenser channels to minimise temperature and concentration polarisation

effects. Key characteristics of the spiral-wound membrane module are summarised in Table 1.
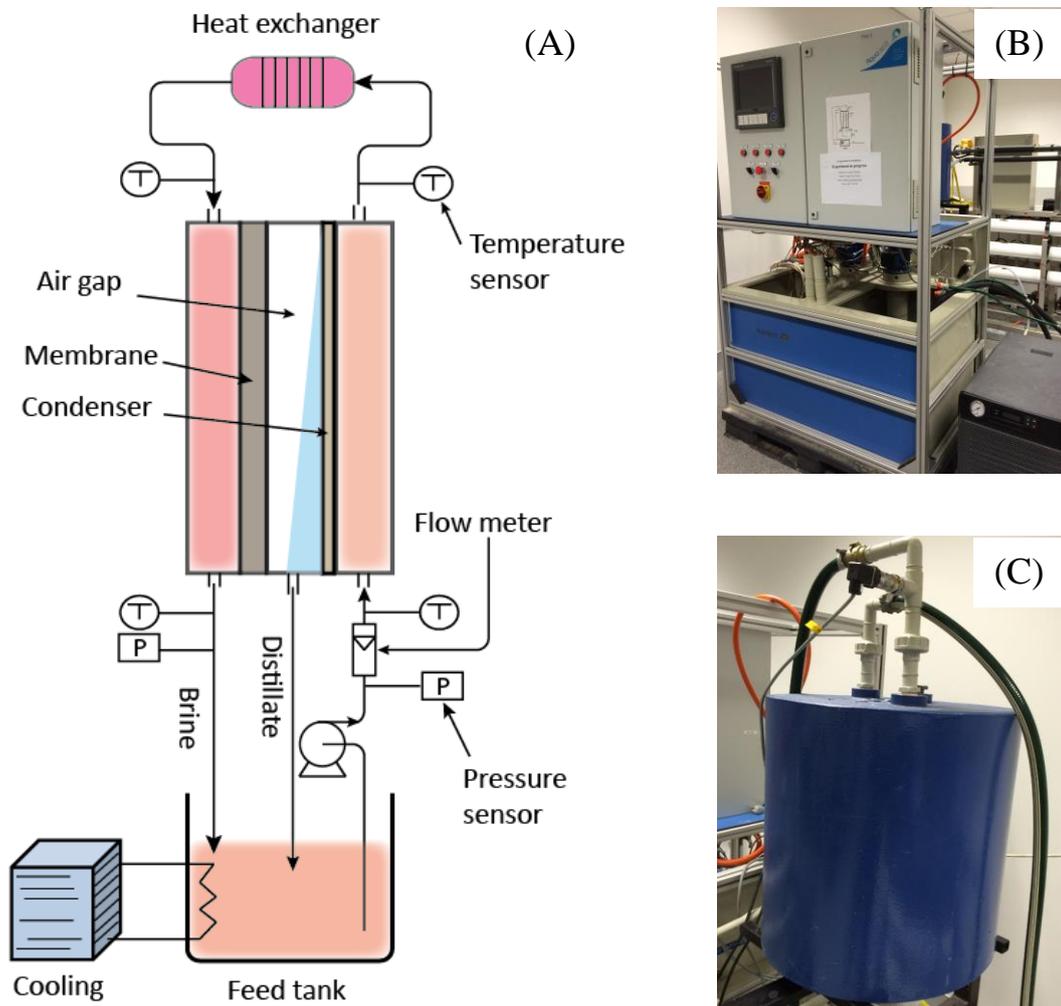


**Fig. 1.** The pilot AGMD system used in the study: (A) a schematic diagram of the system, (B) a photograph of the pilot system, and (C) a photograph of the spiral-wound AGMD membrane module.

**Table 1.** Characteristics of the spiral-wound AGMD membrane module.

| | |
|---|---|
| Effective membrane surface area (m$^2$) | 7.2 |
| Diameter of the module (m) | 0.4 |
| Height of the module (m) | 0.5 |
| Length of envelope (m) | 1.5 |
| Width of envelope (m) | 0.4 |
| Thickness of the evaporator channels (mm) | 2.0 |
| Thickness of the condenser channels (mm) | 2.0 |
| Thickness of the distillate channels (mm) | 1.0 |
| Number of evaporator channels | 6 |
| Number of condenser channels | 6 |
| Number of distillate channels | 12 |

The spiral-would AGMD membrane module had been designed specifically to recover the latent heat of condensation. Briefly, saline solution from the feed tank first entered the condenser channels of the membrane module to primarily function as the coolant. When the saline feed solution (coolant) was flowing along the condenser channels, it facilitated the condensation of water vapour that crossed the membranes from the evaporator channels, and simultaneously was pre-heated. The pre-heated saline solution leaving the condenser channels was further heated using an external heat exchanger. The heated saline solution was then fed into the evaporator channels, where water vapour was formed and diffused across the membranes to the distillate channels. The warm concentrate (i.e., the brine) leaving the evaporator channels was returned to the feed tank. To simulate single-pass operation, the distillate was also returned to the feed tank, and a cooler was employed to maintain the constant temperature of the saline solution in the feed tank (Fig. 1).

Temperatures of the process stream at the inlet and outlet of the condenser and evaporator channels were measured using four temperature sensors. The hydraulic pressure drop along the spiral-wound membrane module was measured using two pressure sensors. A magnetic flow meter was placed before the inlet of the condensers channels to measure the water circulation rate. The temperature and pressure sensors and the flow meter were connected to the supervisory control and data acquisition system of the pilot system for continuous measurement and data recording. Electrical conductivity of the feed and the distillate was measured using Orion 4-Star Plus meters (Thermo Scientific, Waltham, Massachusetts, USA). Distillate production rate of the process was measured using a 500 mL gradual cylinder and a stopwatch.

### 2.1.2. Feed solutions

Tap water, synthetic NaCl solution, and seawater were used as feed solutions. Seawater was collected from Bulli beach (New South Wales, Australia) and was used without any pre-treatment. The seawater had electrical conductivity, pH, and total dissolved solids of $55.0 \pm 0.5$ mS/cm, $8.35 \pm 0.05$, and $35,000 \pm 250$ mg/L, respectively. The total organic carbon (TOC) concentration of this seawater was less than 2 mg/L. The synthetic NaCl solution having a similar salinity to the seawater (i.e., 35,000 mg/L) was prepared from analytical grade chemical and tap water.

### 2.2. Experimental protocols

#### 2.2.1. Pilot AGMD of tap water and of synthetic NaCl solution

Pilot AGMD of tap water was conducted to characterise the performance of the pilot system. To simulate the single-pass AGMD of seawater, the condenser inlet temperature, $T_{c.in}$, was remained at 25 ℃, while the evaporator inlet temperature, $T_{e.in}$, was varied from 50 to 70 ℃. The water circulation rate ($F_{feed}$) was in the range from 150 to 350 L/h, which was the permissible range of the pilot system. The distillate production rate ($F_{dist}$), evaporator inlet and outlet temperatures, condenser inlet and outlet temperatures, and the hydraulic pressures at the inlet and outlet of the membrane module were measured and recorded when the process had been at stable conditions for 1 hour.

Pilot AGMD evaluation of the synthetic NaCl solution feed was conducted under the same operating conditions as described above to elucidate the influence of feed salinity on the distillate production rate and specific thermal and electrical energy consumption of the process. In addition to distillate production rate and temperatures and hydraulic pressures of the process streams, conductivities of the distillate and the NaCl solution in the feed tank were regularly measured.

#### 2.2.2. Pilot AGMD of seawater

The optimum evaporator inlet temperature and water circulation rate (i.e., with regard to specific thermal and electrical energy consumption), which were obtained from the experiment with the NaCl solution feed, were used to evaluate the AGMD operation with seawater feed. The purpose of this experiment was to demonstrate a stable single-pass AGMD desalination of seawater with minimal energy consumption. A batch of 500 L of seawater was used for one pilot operation. The operation was maintained for 9 hours under stable operating conditions. Distillate production rate, temperatures and hydraulic pressures of the process streams, and conductivities of the seawater feed and the distillate were recorded every hour.

### 2.3. Electrical energy consumption and thermal efficiency calculations

In the MD process, electrical energy and thermal energy are required for water circulation and phase conversion, respectively. The electrical energy consumption of the pilot system

was evaluated using specific electrical energy consumption (*SEEC*), which is the electrical energy consumed per volume unit of distillate produced (kWh/m$^3$). The *SEEC* of the pilot AGMD system was calculated using Eq. 1 [21]:

$$SEEC = \frac{F_{feed} \times \Delta P_{drop}}{36 \times \eta \times F_{dist}} \tag{1}$$

where $F_{feed}$ and $F_{dist}$ are the water circulation rate and distillate production rate (L/h), respectively, $\Delta P_{drop}$ is the hydraulic pressure drop over the AGMD module (bar), and $\eta$ is the efficiency of the water-circulating pump.

In this study, the warm brine stream leaving the evaporator channels was returned to the feed tank, thus cooling was required to maintain the constant condenser inlet temperature. However, in practice, seawater can be used as the coolant and the warm brine stream can be discharged from the single-pass AGMD process. Thermal energy is only required to further heat the feed stream prior to the evaporator inlet to generate the process driving force. As a result, the specific thermal energy consumption (*STEC*) of the pilot system, which is the amount of thermal energy required per volume unit of distillate produced (kWh/m$^3$), was calculated as:

$$STEC = \frac{F_{feed} \times \rho_{feed} \times C_p \times \Delta T_{top}}{3.6 \times 10^6 \times F_{dist}} \tag{2}$$

where $\rho_{feed}$ and $C_p$ are the density (kg/m$^3$) and specific heat capacity (J/kg.K) of the feed stream, respectively, and $\Delta T_{top}$ is the temperature difference between the evaporator inlet and the condenser outlet.

In addition to *STEC*, gained output ratio (*GOR*), which is a ratio between the useful heat (i.e., the heat associated with water vapour transfer) and the total heat input of the system, was used to evaluate the thermal efficiency of the pilot process. *GOR* indicates how efficient the MD system is in terms of heat recovery, and can be calculated as:

$$GOR = \frac{10^3 \times F_{dist} \times \rho_{dist} \times \Delta H}{F_{feed} \times \rho_{feed} \times C_p \times \Delta T_{top}} \tag{3}$$

where $\rho_{dist}$ is the density of the distillate (kg/m$^3$) and $\Delta H$ is the latent heat of evaporation of water (kJ/kg).

## 3. Results and discussions

### 3.1. Characterisation of the pilot AGMD system with tap water

*3.1.1. Influence of evaporator inlet temperature on the performance of the system*

In this study, the temperature difference between the evaporator inlet and the condenser outlet ($\Delta T_{top}$) was up to 0.8 ℃ higher than that between the evaporator outlet and the condenser inlet ($\Delta T_{bottom}$). However, for simplicity, the average value of $\Delta T_{top}$ and $\Delta T_{bottom}$, denoted as $\Delta T$, is presented when considering the driving force of the process.

When operating at an increased feed (evaporator inlet) temperature, the AGMD system could achieve a higher distillate production rate. Indeed, the distillate production rate increased from 4.5 to 9.5 L/h when the evaporator inlet temperature increased from 50 to 70 ℃ (Fig. 2). This observed increase in the distillate production rate can be attributed to the larger water vapour pressure difference across the membrane at an elevated temperature, as predicted by the Antoine equation [22]. In addition, the increase in the evaporator inlet temperature also led to an increase in the driving force of the process (i.e., $\Delta T$ increased from 2.0 to 3.0 ℃).

Operating the system at a high feed temperature also increased the thermal efficiency of the AGMD process. The system specific thermal energy consumption (*STEC*) decreased from 82 to 67 kWh/m$^3$ when the evaporator inlet temperature increased from 50 to 70 ℃ (Fig. 2). Similarly, the system gained output ratio (*GOR*) increased from 7.5 to 9.5 with the increase in the evaporator inlet temperature. The observed improvement in thermal efficiency at high feed temperature can also be explained by the relationship between water vapour pressure and temperature according to the Antoine equation as noted above. The benefit of operating the process at a high feed temperature with regard to thermal efficiency has been reported for other MD configurations [23, 24].

The increase in feed temperature also led to a small, but noticeable reduction in the specific electrical energy consumption (*SEEC*). This is mostly driven by the increase in the

distillate production rate while the electrical energy demand for water circulation remained constant at the unchanged water circulation rate (Fig. 2).
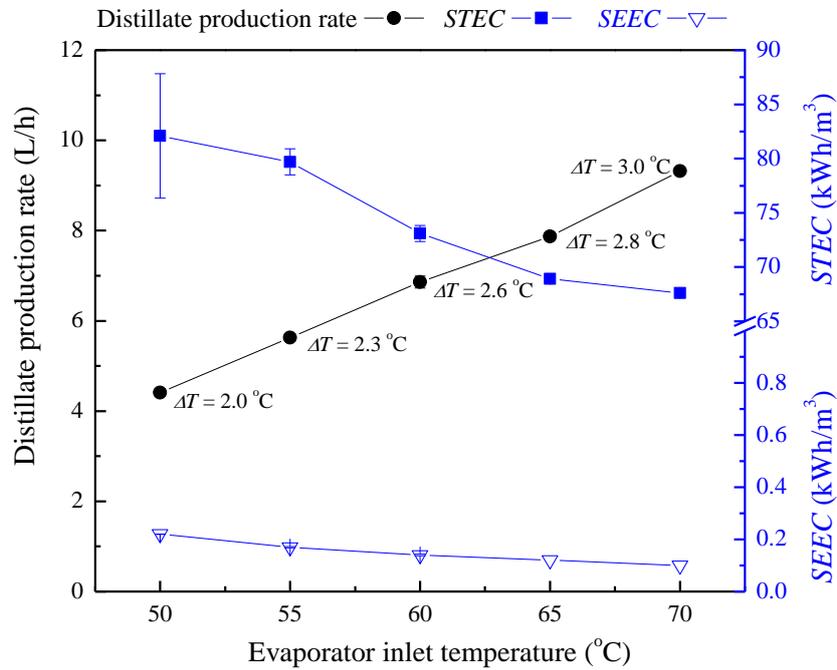


**Fig. 2.** Distillate production rate, *STEC*, and *SEEC* as functions of evaporator inlet temperature in pilot AGMD of tap water. Other operating conditions: $T_{c.in}$ = 25 ℃, $F_{feed}$ = 150 L/h. Error bars represent the standard deviation of triplicate experiments.

### 3.1.2. Influence of water circulation rate on the performance of the system

The distillate production rate could also be increased by increasing water circulation rate within the membrane module (Fig. 3). Increasing the water circulation rate from 150 to 350 L/h resulted in an increase in *ΔT* from 3.0 to 4.5 ℃; thus, the distillate production rate increased from 9.5 to 19 L/h. The positive influence of water circulation rate on permeate flux, and thus distillate production rate in MD, has been widely reported [23, 25-27]. However, it is important to note that these previous studies used lab-scale DCMD systems with a high permeate flux induced by a large driving force (*ΔT* > 25 ℃). Thus, the effects of temperature and concentration polarisation were significant [18, 23]. Increasing water circulation rate helped reduce the temperature and concentration polarisation effects, and hence improved permeate flux. In this pilot AGMD study, the driving force was small (*ΔT* <

5 ℃) and thus the polarisation effects were rather small. As a result, the observed increase in distillate production rate can be mostly attributed to the increased $\Delta T$ (Fig. 3).
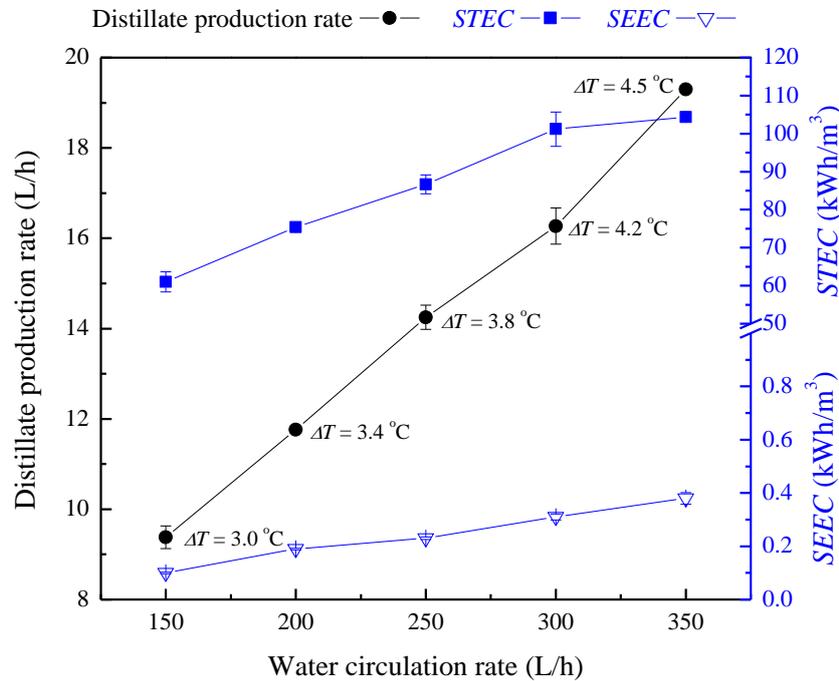


**Fig. 3.** Distillate production rate, *STEC*, and *SEEC* as functions of water circulation rate in the pilot AGMD of tap water feed. Other operating conditions: $T_{c.in} = 25$ ℃, $T_{e.in} = 70$ ℃. Error bars represent the standard deviation of triplicate experiments.

The role of temperature polarisation effect in the pilot AGMD process at different operating conditions can be clarified by examining the distillate production rate as a function of $\Delta T$ (Fig. 4). Elevating the feed temperature or the water circulation rate both led to an increase in $\Delta T$, and thus increased permeate flux. Increasing permeate flux magnifies the temperature polarisation effect [26, 28]. However, unlike feed temperature, increasing the water circulation rate also helped mitigate the negative effect of temperature polarisation [28, 29]. As a result, the slope of distillate production rate against $\Delta T$ for the set of water circulation rate experiments was slightly higher compared to the feed temperature experiments (Fig. 4). It is noteworthy that operating temperature might also affect the slope. Thus, further studies on the influence of operating conditions on polarisation effects during pilot AGMD are recommended.
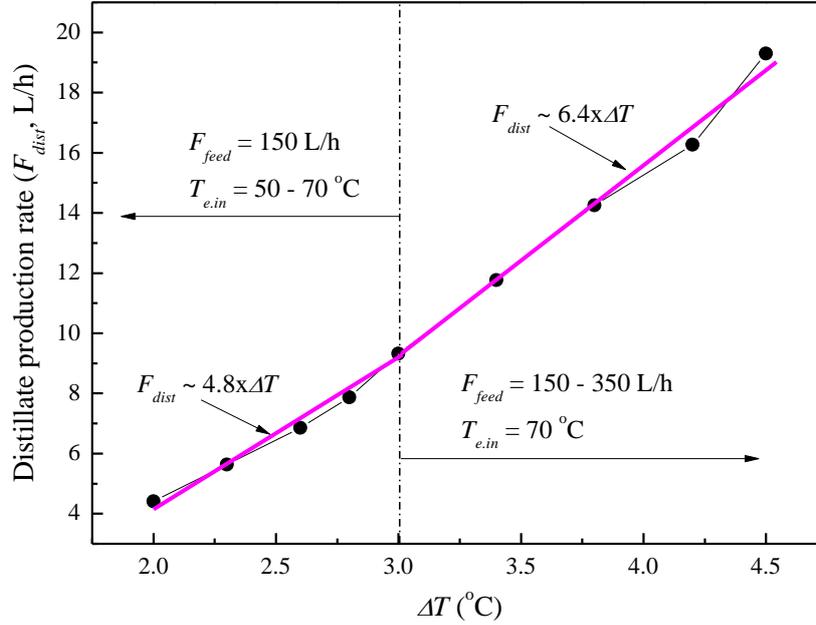
**Fig. 4.** Distillate production rate ($F_{dist}$) as a function of the driving force ($\Delta T$) when the evaporator inlet temperature or water circulation rate increased in the pilot AGMD of tap water. Error bars represent the standard deviation of triplicate experiments.

Operating the pilot process at a high water circulation rate resulted in a low thermal efficiency. Increasing the water circulation rate reduced the residence time of the coolant and the hot feed inside the membrane module, thus, reducing the heat recovery efficacy. In other words, the recovery of latent heat from the water vapour to the coolant decreased, leading to an increase in $\Delta T_{top}$. Elevated water circulation rate and the associated increase in $\Delta T_{top}$ resulted in an increase in the total heat input into the system (Eq. 2). The total heat input increased at a higher rate compared to the distillate production rate when the water circulation rate increased. As a result, the *STEC* of the system increased from 65 to 105 kWh/m$^3$ when the water circulation rate was elevated from 150 to 350 L/h (Fig. 3). Correspondingly, the *GOR* of the system decreased from 9.5 to 6.0. A similar influence of water circulation rate on thermal efficiency was also reported for DCMD with brine recycling [24] and when employing an external heat-exchanger [30, 31].

The water circulation rate also exerted a strong influence on the *SEEC* of the system. The *SEEC* of the system is proportional to the water circulation rate ($F_{feed}$) and the hydraulic pressure drop over the membrane module ($\Delta P_{drop}$) according to Eq. 1. Increasing the water

circulation rate from 150 to 350 L/h resulted in an increase in $\Delta P_{drop}$ from 0.14 to 0.45 bar. As a result, the *SEEC* of the system significantly increased (i.e., from 0.1 to 0.4 kWh/m$^3$) despite the increase in distillate production rate (Fig. 3).

## 3.2. Influence of feed salinity on the performance of the pilot system

The presence of NaCl (35,000 mg/L) in the feed solution significantly reduced the distillate production rate of the pilot AGMD compared to the reference experiments using tap water feed (Fig. 5). Dissolved NaCl in the feed solution decreases water activity, and thus reduces the transmembrane partial water vapour pressure, which is the actual driving force of the MD process [22]. Indeed, using the Antoine equation [22], the actual driving force of the pilot AGMD with the NaCl solution feed (i.e., with evaporator inlet temperature and water circulation rate of 50 ℃ and 150 L/h, respectively, and an assumed temperature polarisation coefficient of 0.7) decreased by 20% compared to the pilot process with tap water feed under the same conditions.
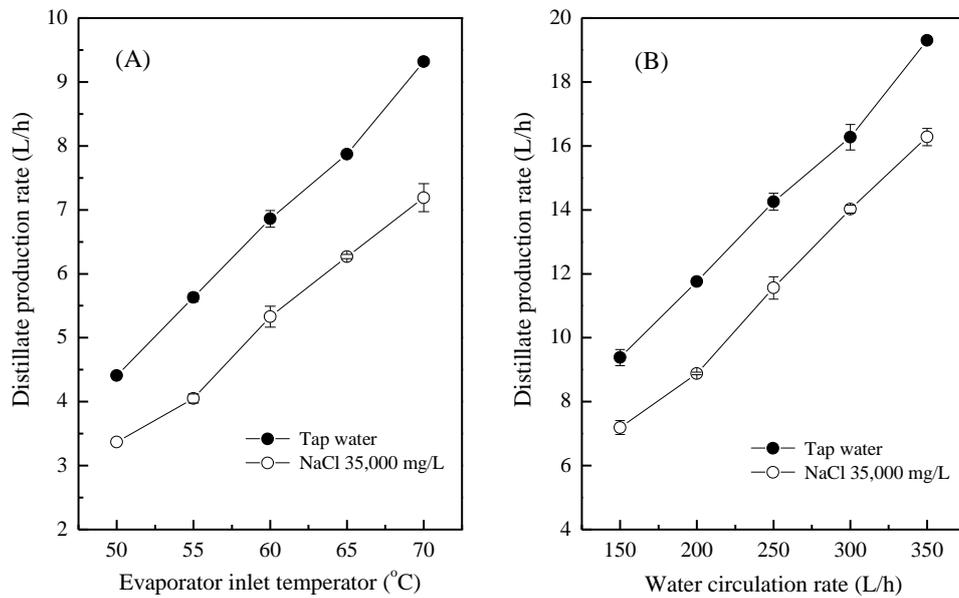


**Fig. 5.** Influence of feed salinity on distillate production rate of the pilot AGMD system at various operating conditions: (A) distillate production rate as a function of evaporator inlet temperature; other operating conditions: $T_{c.in}$ = 25 ℃, $F_{feed}$ = 150 L/h, and (B) distillate production rate as a function of water circulation rate; other operating conditions: $T_{c.in}$ = 25 ℃, $T_{e.in}$ = 70 ℃. Error bars represent the standard deviation of triplicate experiments.

In addition to decreased water activity, concentration polarisation effect might also cause a reduction in the distillate production rate when using a saline feed. Elevating the feed temperature with a constant water circulation rate increased the concentration polarisation effect [29]. Thus, the decline in the distillate production rate in the process of saline solution feed, compared to that of tap water feed, was more significant at a higher feed temperature (Fig. 5A). On the contrary, the effect of concentration polarisation in the process of saline solution feed was indiscernible when the water circulation rate changed (Fig. 5B). Increasing the water circulation rate mitigated the effect of concentration polarisation because of increased flow turbulence; however, it also exaggerated the concentration polarisation effect due to the associated increase in permeate flux.

The influences of operating conditions on the specific energy consumption of the pilot AGMD process with the NaCl solution feed were similar to those observed in the experiment with tap water feed (Fig. 6). Elevating the evaporator inlet temperature and decreasing the water circulation rate also reduced the *STEC* and *SEEC* of the pilot process when operating with the NaCl feed solution. However, the presence of salts in the feed solution increased both *STEC* and *SEEC* because of the decreased distillate production rate compared to the reference results using tap water (Figs. 5 and 6).
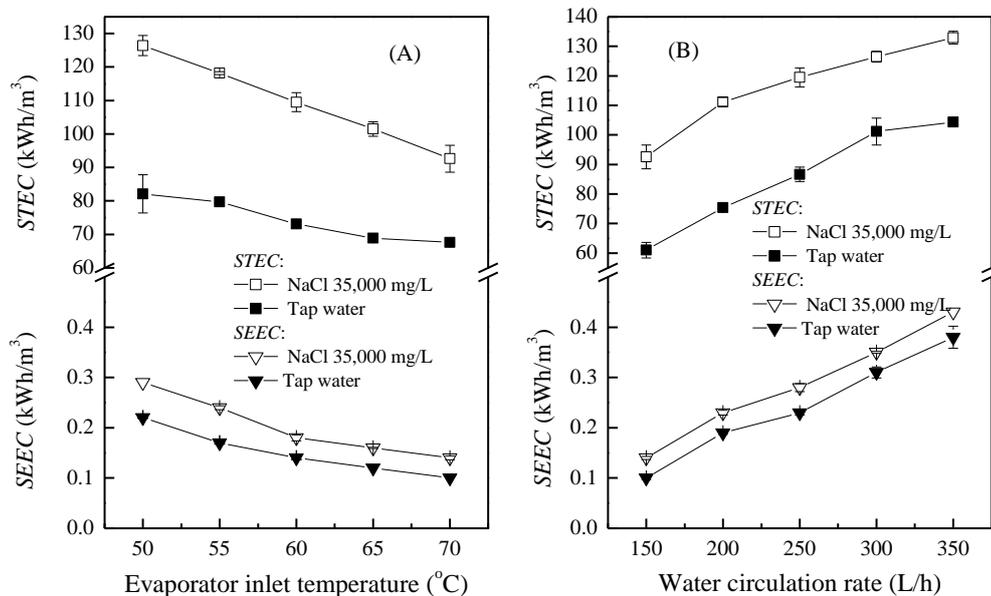


**Fig. 6.** Influence of feed salinity on the specific thermal and electrical energy consumption of the pilot AGMD system at various operating conditions: (A) *STEC* and *SEEC* as a function of evaporator inlet temperature, other operating conditions: $T_{c.in}$ = 25 ℃, $F_{feed}$ = 150 L/h, and

14

(B) *STEC* and *SEEC* as a function of water circulation rate; other operating conditions: $T_{c.in}$ = 25 ℃, $T_{e.in}$ = 70 ℃. Error bars represent the standard deviation of triplicate experiments.

### 3.3. Pilot AGMD process of seawater

The evaporator inlet temperature of 70 ℃ and the water circulation rate of 150 L/h were the optimal operating conditions (i.e., with respect to specific energy consumption) in the pilot process with tap water and the saline solution feed. Thus, these conditions were selected for further experiment with seawater.

A stable pilot AGMD operation with seawater feed and without any pre-treatment was obtained. Throughout 9 hours of operation, the distillate production rate of the system remained steady at 7.3 L/h (Fig. 7), and the distillate conductivity was always below 100 μS/cm (i.e., equivalent to the salinity of 50 mg/L). The stable distillate production rate and distillate conductivity confirm the absence of membrane scaling and fouling during the operation. It is noteworthy that in the single-pass operation, the water recovery rate of the pilot AGMD system was noticeably low (i.e., 5%). Low water recovery rate together with a small concentration polarisation ensured that concentrations of potential scalants, such as $CaCO_3$ and $CaSO_4$ [24, 32, 33], at the membrane surface were well below their solubility limits. The stable distillate production rate (which indicates the absence of any membrane fouling) observed in this experiment can be also attributed to the low total organic carbon concentration of the seawater feed (i.e., <2 mg/L) and low operating permeate flux (i.e., 1.0 L/m²-h). The results reported here are consistent with previous studies, in which MD was reported to be able to desalt seawater without any intensive chemical pre-treatment for months of operation [34, 35].
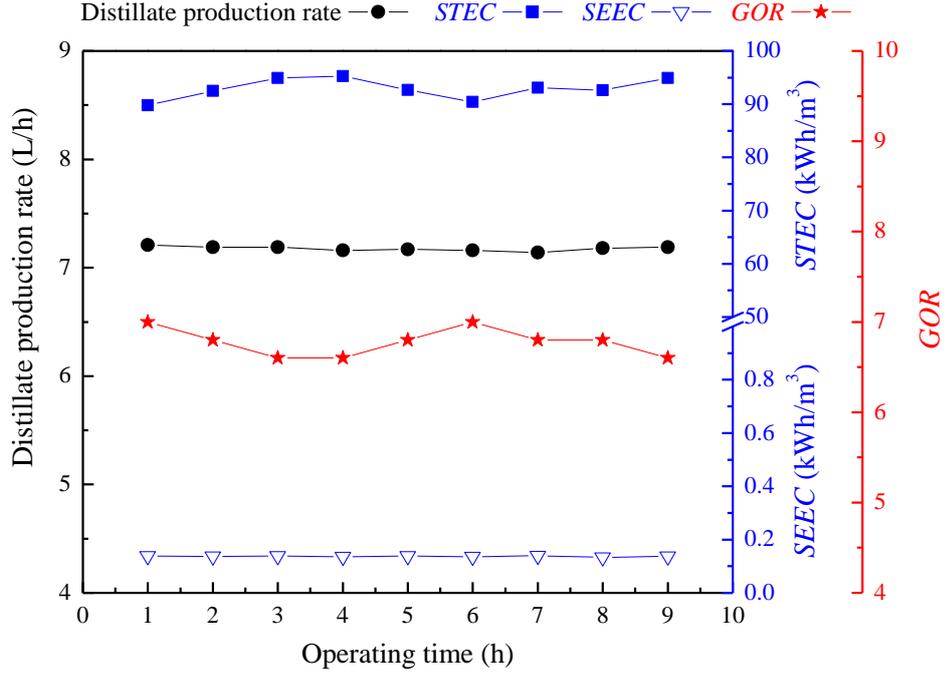
**Fig. 7.** Distillate production rate, *STEC*, *SEEC*, and *GOR* as functions of operating time in the pilot AGMD treatment of seawater. Operating conditions: $T_{c.in}$ = 25 °C, $T_{e.in}$ = 70 °C, $F_{feed}$ = 150 L/h.

Throughout the experiment, the *STEC* and *GOR* of the system slightly varied from 90 to 95 kWh/m$^3$ and 6.5 to 7, respectively, while the *SEEC* of the system remained stable at 0.13 kWh/m$^3$ (Fig. 7). The variations in *STEC* and *GOR* were attributed to the fluctuation in the value of $\Delta T_{top}$, which was inevitable for the pilot system. Differently, the factors determining the *SEEC* of the system remained stable; thus, a constant *SEEC* was obtained. It is also noteworthy that the distillate production rate obtained from seawater is similar to that from a 35,000 mg/L NaCl solution reported in section 3.2.

Compared to a state-of-the-art seawater RO process, the pilot AGMD process had a significantly lower *SEEC* (i.e., 0.13 compared to approximately 4 kWh/m$^3$) [14]. This comparison roughly demonstrates the advantage of MD over RO for seawater desalination when integrating with solar energy. PV panels used to supply electrical energy to solar-driven desalination systems contribute a significant portion to the capital costs of the systems [10, 14]. The operational costs of MD can also be reduced when using low-grade waste heat available on site. Indeed, water production cost as low as 0.26 \$/m$^3$ has been reported for a seawater MD desalination unit using waste heat [36].

Comparisons between the pilot AGMD system used in the present study and other pilot AGMD systems reported in the literature are provided in Table 2. Under the optimal operating conditions (i.e., the evaporator inlet temperature and water circulation rate), our system achieved the lowest *STEC* and the highest *GOR*. However, the permeate flux of the present system was also the lowest. It is noteworthy that while the evaporator inlet temperature used in the present study was in the range investigated in previous studies, the water circulation rate was much lower in the present experiments. This again confirms the strong influence of water circulation rate on permeate flux and energy consumption of AGMD systems.

**Table 2.** Comparisons between the thermal and electrical energy consumption of the pilot AGMD system in this study and values previously reported in the literature.

| | Present study | Literature | | | |
|---|---|---|---|---|---|
| | | [10] | [34] | [12] | [11] |
| Water circulation flow rate (L/h) | 150 | 280-415 | 400 | 500 | 200-400 |
| Feed temperature at evaporator inlet ($^{\circ}$C) | 70 | 60-85 | - | 85 | 60-85 |
| Permeate flux (L/m$^2$-h) | 1.0 | 2.1 | 2.5 | 3.4 | 1.88 |
| *STEC* (kWh/m$^3$) | 90-95 | 100-200 | 200-300 | 250-600 | 140-200 |
| *SEEC* (kWh/m$^3$) | 0.13 | - | - | - | - |
| *GOR* | 6-7 | 3-6 | 0.3-0.9 | - | 4-6 |

## 4. Conclusions

We investigated the optimisation of a single-pass pilot AGMD process of seawater with respect to distillate production rate and energy consumption. The evaporator inlet temperature and the water circulation rate strongly influenced the process performance. The process delivered a better performance (i.e., higher distillate production rate and lower specific thermal and electrical energy consumption) when operating at elevated evaporator inlet temperature. In contrast, a trade-off between the distillate production rate and energy efficiency of the process was observed as the water circulation rate increased. Furthermore, given the small driving force ($\Delta T < 5$ $^{\circ}$C) used in this study, both temperature and concentration polarisation effects of the AGMD process were rather small. On the other hand, the effects of feed salinity (which resulted in a decrease in water activity and an increase in concentration polarisation) on distillate production rate and thermal efficiency were clearly discernible. Finally, a stable single-pass pilot AGMD operation of seawater with a specific thermal and electrical energy consumption of 90 and 0.13 kWh/m$^3$, respectively, was

demonstrated. The specific thermal energy consumption obtained here is lower than all other values from previous pilot AGMD evaluations in the literature.

## Acknowledgements

## References

[1]   M. Elimelech and W.A. Phillip, The Future of Seawater Desalination: Energy, Technology, and the Environment, Science 333 (2011) 712-717.

[2]   N. Ghaffour, J. Bundschuh, H. Mahmoudi, and M.F.A. Goosen, Renewable energy-driven desalination technologies: A comprehensive review on challenges and potential applications of integrated systems, Desalination 356 (2015) 94-114.

[3]   A. Chafidz, S. Al-Zahrani, M.N. Al-Otaibi, C.F. Hoong, T.F. Lai, and M. Prabu, Portable and integrated solar-driven desalination system using membrane distillation for arid remote areas in Saudi Arabia, Desalination 345 (2014) 36-49.

[4]   W.G. Shim, K. He, S. Gray, and I.S. Moon, Solar energy assisted direct contact membrane distillation (DCMD) process for seawater desalination, Sep. Purif. Technol. 143 (2015) 94-104.

[5]   A. Kullab and A. Martin, Membrane distillation and applications for water purification in thermal cogeneration plants, Sep. Purif. Technol. 76 (2011) 231-237.

[6]   E. Drioli, A. Ali, and F. Macedonio, Membrane distillation: Recent developments and perspectives, Desalination 356 (2015) 56-84.

[7]   A. Alkhudhiri, N. Darwish, and N. Hilal, Membrane distillation: A comprehensive review, Desalination 287 (2012) 2-18.

[8]   M. Khayet, Solar desalination by membrane distillation: Dispersion in energy consumption analysis and water production costs (a review), Desalination 308 (2013) 89-101.

[9]   S. Adham, A. Hussain, J.M. Matar, R. Dores, and A. Janson, Application of membrane distillation for desalting brines from thermal desalination plants, Desalination 314 (2013) 101-108.

[10]  J. Koschikowski, M. Wieghaus, M. Rommel, V.S. Ortin, B.P. Suarez, and J.R. Betancort Rodríguez, Experimental investigations on solar driven stand-alone membrane distillation systems for remote areas, Desalination 248 (2009) 125-131.

[11]  J. Koschikowski, M. Wieghaus, and M. Rommel, Solar thermal-driven desalination plants based on membrane distillation, Desalination 156 (2003) 295-304.

[12]  G. Zaragoza, A. Ruiz-Aguirre, and E. Guillén-Burrieza, Efficiency in the use of solar thermal energy of small membrane desalination systems for decentralized water production, Appl. Energy 130 (2014) 491-499.

[13]  J.-P. Mericq, S. Laborie, and C. Cabassud, Evaluation of systems coupling vacuum membrane distillation and solar energy for seawater desalination, Chem. Eng. J. 166 (2011) 596-606.

[14]  A. Al-Karaghouli and L.L. Kazmerski, Energy consumption and water production cost of conventional and renewable-energy-powered desalination processes, Renew. Sust. Energ. Rev. 24 (2013) 343-356.

[15]  E. Guillén-Burrieza, G. Zaragoza, S. Miralles-Cuevas, and J. Blanco, Experimental evaluation of two pilot-scale membrane distillation modules used for solar desalination, J. Membr. Sci. 409–410 (2012) 264-275.

[16]  R.B. Saffarini, E.K. Summers, H.A. Arafat, and J.H. Lienhard V, Technical evaluation of stand-alone solar powered membrane distillation systems, Desalination 286 (2012) 332-341.

[17]  J. Minier-Matar, A. Hussain, A. Janson, F. Benyahia, and S. Adham, Field evaluation of membrane distillation technologies for desalination of highly saline brines, Desalination 351 (2014) 101-108.

[18]  H.C. Duong, A.R. Chivas, B. Nelemans, M. Duke, S. Gray, T.Y. Cath, and L.D. Nghiem, Treatment of RO brine from CSG produced water by spiral-wound air gap membrane distillation - A pilot study, Desalination 366 (2015) 121-129.

[19]  A.S. Alsaadi, L. Francis, H. Maab, G.L. Amy, and N. Ghaffour, Evaluation of air gap membrane distillation process running under sub-atmospheric conditions: Experimental and simulation studies, J. Membr. Sci. 489 (2015) 73-80.

[20]  P. Wang and T.-S. Chung, Recent advances in membrane distillation processes: Membrane development, configuration design and application exploring, J. Membr. Sci. 474 (2015) 39-56.

[21]  I.J. Karassik, J.P. Messina, P. Cooper, and C.C. Heald, Pump Handbook, Third edition, McGraw-Hill, USA, 2001, pp . 1-1790.

[22]  K.W. Lawson and D.R. Lloyd, Membrane distillation, J. Membr. Sci. 124 (1997) 1-25.

[23]  S. Al-Obaidani, E. Curcio, F. Macedonio, G. Di Profio, H. Al-Hinai, and E. Drioli, Potential of membrane distillation in seawater desalination: Thermal efficiency, sensitivity study and cost estimation, J. Membr. Sci. 323 (2008) 85-98.

[24]  H.C. Duong, P. Cooper, B. Nelemans, and L.D. Nghiem, Optimising thermal efficiency of direct contact membrane distillation via brine recycling for small-scale seawater desalination, Desalination 374 (2015) 1-9.

[25] J. Zhang, S. Gray, and J.-D. Li, Predicting the influence of operating conditions on DCMD flux and thermal efficiency for incompressible and compressible membrane systems, Desalination 323 (2013) 142-149.

[26] P. Termpiyakul, R. Jiraratananon, and S. Srisurichan, Heat and mass transfer characteristics of a direct contact membrane distillation process for desalination, Desalination 177 (2005) 133-141.

[27] Z. Song, L. Li, H. Wang, B. Li, and S. Wang, DCMD flux curve characteristics of cross-flow hollow fiber membrane, Desalination 323 (2013) 107-113.

[28] L. Martínez-Díez, F.J. Florido-Díaz, and M.I. Vázquez-González, Study of evaporation efficiency in membrane distillation, Desalination 126 (1999) 193-198.

[29] L. Martínez-Díez and M.I. Vázquez-González, Temperature and concentration polarization in membrane distillation of aqueous salt solutions, J. Membr. Sci. 156 (1999) 265-273.

[30] E.K. Summers, H.A. Arafat, and J.H. Lienhard V, Energy efficiency comparison of single-stage membrane distillation (MD) desalination cycles in different configurations, Desalination 290 (2012) 54-66.

[31] G. Guan, X. Yang, R. Wang, and A.G. Fane, Evaluation of heat utilization in membrane distillation desalination system integrated with heat recovery, Desalination 366 (2015) 80-93.

[32] L.D. Nghiem, F. Hildinger, F.I. Hai, and T. Cath, Treatment of saline aqueous solutions using direct contact membrane distillation, Desalin. Water Treat. 32 (2011) 234-241.

[33] P. Zhang, P. Knötig, S. Gray, and M. Duke, Scale reduction and cleaning techniques during direct contact membrane distillation of seawater reverse osmosis brine, Desalination 374 (2015) 20-30.

[34] F. Banat, N. Jwaied, M. Rommel, J. Koschikowski, and M. Wieghaus, Desalination by a "compact SMADES" autonomous solar-powered membrane distillation unit, Desalination 217 (2007) 29-37.

[35] R.G. Raluy, R. Schwantes, V.J. Subiela, B. Peñate, G. Melián, and J.R. Betancort, Operational experience of a solar membrane distillation demonstration plant in Pozo Izquierdo-Gran Canaria Island (Spain), Desalination 290 (2012) 1-13.

[36] G.W. Meindersma, C.M. Guijt, and A.B. de Haan, Desalination and water recycling by air gap membrane distillation, Desalination 187 (2006) 291-301.